A stand-alone magnetic guide for producing tuneable radical beams

Chloé Miossec,[1, a)] Lok Yiu Wu,[1, a)] Paul Bertier,[1] Michal Hejduk,[1] Jutta Toscano,[2] and Brianna R. Heazlewood[1]

[1)]*Physical and Theoretical Chemistry Laboratory, University of Oxford, South Parks Road, Oxford, OX1 3QZ, UK*

[2)]*JILA and Department of Physics, University of Colorado, Boulder, Colorado 80309, USA*

(Dated: 22 August 2020)

Radicals are prevalent in gas-phase environments such as the atmosphere, combustion systems and the interstellar medium. To understand the properties of the processes occurring in these environments, it is helpful to study radical reaction systems in isolation—thereby avoiding competing reactions from impurities. There are very few methods for generating a pure beam of gas-phase radicals, and those that do exist involve complex set-ups. Here, we provide a straightforward and versatile solution. A magnetic radical filter (MRF), composed of four Halbach arrays and two skimming blades, can generate a beam of velocity-selected low-field-seeking hydrogen atoms. As there is no line-of-sight through the device, all species that are unaffected by the magnetic fields are physically blocked; only the target radicals are successfully guided around the skimming blades. The positions of the arrays and blades can be adjusted, enabling the velocity distribution of the beam (and even the target radical species) to be modified. The MRF is employed as a stand-alone device—filtering radicals directly from the source. Our findings open up the prospect of studying a range of radical reaction systems with a high degree of control over the properties of the radical reactants.

[a)]These authors contributed equally

I. INTRODUCTION

Radicals are abundant in gas-phase environments—they are present in the atmosphere, the interstellar medium, combustion environments, even in our breath. Understanding how radicals react is therefore relevant for a vast array of multi-disciplinary fields, including atmospheric chemistry, interstellar modelling, industrial processes and the healthcare industry. In spite of their prevalence and importance, there have been very few precise gas-phase studies of processes involving radical reactants. This lack of experimental scrutiny can be attributed to the significant challenges associated with preparing a pure and controllable source of radical reactants; there are no straightforward methods for generating a pure beam of state-selected atomic or molecular gas-phase radicals with tuneable properties.

Gas-phase radicals are readily formed by photolysis, electron beam irradiation or electric discharge methods,[1–3] and as such a number of other (unwanted) species are typically present in the beam. It is the filtering of these radicals—the removal of all unwanted species from the beam—that is experimentally challenging. Scientists have been using external magnetic fields in an attempt to manipulate and control beams of paramagnetic particles (radicals) for many decades. Stern, Gerlach, Rabi and Ramsey (amongst others) were early pioneers in the use of inhomogeneous magnetic fields to deflect the paramagnetic components of a beam.[4–8] This is because radicals in low-field-seeking (LFS) quantum states experience an increase in potential energy in the presence of an external magnetic field, enabling the LFS radicals to be separated from other components of a beam. In a 1980 theory paper, Halbach set out the design of a magnetic guide based on an arrangement of permanent multipole magnets.[9] Building upon this foundation, the construction of a curved guide containing an assembly of multipole magnets was experimentally achieved in 1999.[10,11] Bent magnetic guides—composed of permanent magnets (as described above) or electromagnets—can filter the radical species of interest from other components of the beam. Forces generated by the Zeeman effect serve to collimate and "guide" the target radicals around the bend; other species are not sufficiently confined by these forces, and so are lost from the beam.

A number of alternative designs have been proposed for bent magnetic guides, including overlapping pairs of quadrupole coils and combining current carrying wires with a series of Halbach arrays.[12–14] The curvature of a bent magnetic guide is fixed, chosen to suit a particular system of interest. As such, there is limited flexibility in the range of radical species that can be guided, and no ability to adjust the velocity range of the transmitted species; a bent guide can only act as

a low-pass velocity filter, and therefore cannot provide continuous tunability in the radical beam velocity. A straight magnetic guide, even when combined with multiple differential pumping stages and preferential focusing of the radical species, typically struggles to remove contaminant species from the beam.[15] Combining a straight magnetic guide (or magnetic hexapole) with a beam stop located on the central beam axis can achieve good state selectivity, with the target radical species making up $\geq 93\%$ of the beam.[16,17] However, magnetic hexapoles offer limited control over the velocity distribution of the radical beam.[17,18] Electrostatic hexapoles that include beam stops or diaphragms have demonstrated excellent state selectivity and offer some tunability—but this approach can only be applied to radicals that also possess an electric dipole (such as OH and NO).[19–21]

A Zeeman decelerator can generate a beam of slow-moving, state-selected paramagnetic species, as first demonstrated in 2007.[22,23] By switching the current applied to a series of solenoid coils (and thus switching the magnetic fields generated within the coils) on and off at carefully synchronised times, the stages of a Zeeman decelerator can progressively remove kinetic energy from target radical species. A number of different Zeeman decelerator designs and switching sequences have been implemented, and a range of radical species have been successfully decelerated.[24–34] However, filtering elements must be added to a Zeeman decelerator to remove all of the non-decelerated species travelling along the main beam axis before the apparatus can be interfaced with a stationary target, such as an ion trap.

A magnetic guide has been demonstrated to successfully filter the beam coming out of a Zeeman decelerator, such that only the Zeeman-decelerated species of interest reach the detection region.[35] Here, we show that the same magnetic guide—termed a Magnetic Radical Filter (MRF)—can operate as a stand-alone device, generating a state-selected and velocity-filtered beam of hydrogen atoms. All contaminant species present in the incoming beam (including seed gas, precursor molecules, other fragments, and H atoms in high-field seeking [HFS] states) are removed by the guide. The MRF has been designed to be combined with an ion trap. Such a combination will enable important gas-phase reactions involving radicals to be examined in isolation (*i.e.*, without competing side reactions) for the first time. Such measurements could provide the missing experimental data needed to improve the accuracy of (for example) complex atmospheric chemistry models—replacing untested predictions from capture theory calculations.

II. METHODS

Hydrogen atoms in the 1s $^2S_{1/2}$ ground electronic state are formed by the photolysis of supersonically-expanded NH_3 seeded in Kr (in a 1:9 ratio). Photolysis takes place in a capillary attached to the face plate of a pulsed valve, enabling the H atoms to undergo further collisions before expanding into the vacuum chamber (see reference[29] for further details on the production of H atoms using this experimental set-up). The resulting hydrogen beam has a broad velocity distribution peaked at around 500 $\mathrm{m\,s^{-1}}$, with the full width at half maximum (FWHM) of the distribution spanning 407–704 $\mathrm{m\,s^{-1}}$. The presence of hydrogen atoms with low initial velocities means that the target species (*i.e.*, LFS H atoms travelling at 300 $\mathrm{m\,s^{-1}}$ or 350 $\mathrm{m\,s^{-1}}$) can be filtered directly—without the need to first decelerate the incoming beam.

In the presence of an external magnetic field, the Zeeman effect splits the energy levels of paramagnetic species. For ground-state hydrogen atoms, the interaction between electron spin ($S = \frac{1}{2}$) and nuclear spin ($I = \frac{1}{2}$) gives rise to hyperfine splitting, resulting in two LFS ($F = 1$, $m_F = +1, 0$) and two HFS ($F = 0$; $F = 1$, $m_F = -1$) states (where F is the total angular momentum and m_F is the projection of F onto the external magnetic field axis). It is the LFS states that are able to be state-selectively manipulated and filtered by the magnetic guide employed in this work.

The magnetic guide has been described in detail elsewhere[35,36] with the key features presented here. The MRF is composed of four hexapole magnets arranged in a Halbach array configuration, along with two skimming blades (see Figure 1). The Halbach arrays are positioned along the beam axis, with a skimming blade located after each pair of arrays. In their optimised configuration for guiding, the centre of each array is offset from the central beam axis. In this way, each pair of arrays deflects and collimates the LFS species in the beam; the first pair directs the target species upwards, with the second pair of arrays returning the species of interest back to the central beam axis. As the skimming blades extend beyond the central beam axis, they break the direct line-of-sight from the source to the detection region.

Only radicals in LFS states (and travelling at a selected velocity) can successfully traverse the guide and avoid the blades. All other particles—radicals travelling at much higher or lower velocities, radicals in HFS states, seed gases, and precursor molecules—are deflected to a lesser extent, are defocused, or are not affected by the magnetic fields. There is a trade-off between achieving a narrow velocity distribution in the post-guide beam and in achieving a high number of state-selected radicals. Increasing the extent to which the blades penetrate the beam axis increases

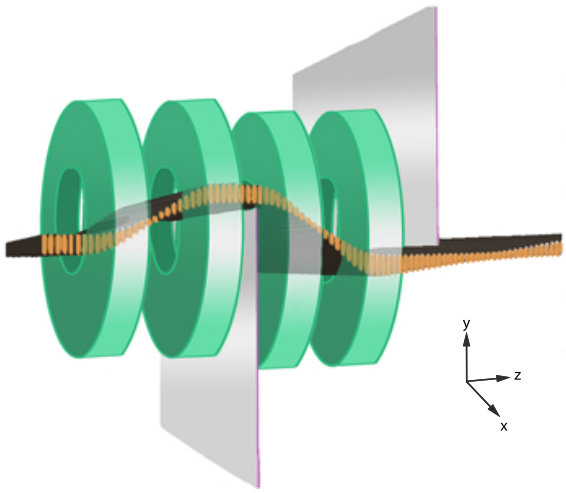

FIG. 1. Schematic illustration of the MRF design. The green cylinders represent the Halbach arrays, where the two arrays within each pair have the same y displacement with respect to the central beam axis. The skimming blades, indicated in silver, overlap in y, preventing any line-of-sight transmission through the guide. The typical trajectories of target particles through the guide are shown; target H atoms are deflected and collimated by each pair of arrays.

the velocity selectivity of the guide, at the expense of the intensity of the transmitted beam. The positions of the blades can be tuned externally (*i.e.*, from outside the vacuum chamber) using micrometre adjustable actuators. One can therefore establish—and adjust—the optimal balance between transmission and velocity distribution during the course of an experiment.

The properties of the species that are preferentially guided by the MRF are determined by the properties of the Halbach arrays (remanence B_0, internal radius r_i, external radius r_e, and thickness l_h) and the relative positions of the arrays. The Halbach arrays employed in this work (B_0 = 1.4 T, r_i = 3 mm, r_e = 7 mm, and l_h = 7 mm) are appropriate for guiding H atoms with velocities spanning 200 to 355 m s^{-1}. The specific target velocity is adjusted by altering the separation between the first and second arrays within each Halbach array pair using a linear actuator. The optimal configuration of the guide elements (*i.e.*, the positions of the arrays and the blades) for preferentially transmitting the target H atoms are determined using three-dimensional particle trajectory simulations. (See reference[35] for a detailed description of the simulations.)

Although we are using the magnetic guide as a stand-alone beam filter, it should be noted that hydrogen atoms have to travel some 24 cm before reaching the MRF. This is due to the physical restrictions of our set-up; the beam is required to traverse a short (12-stage) Zeeman decelerator

(with no fields applied to the coils) before it reaches the start of the MRF. Although the decelerator is not in operation, the increased path length significantly reduces the number of particles from the initial beam that reach the guide. All of these details are accounted for in the particle trajectory simulations.

III. RESULTS AND DISCUSSION

Figure 2 presents the Time-of-Flight (ToF) traces recorded using resonance-enhanced multi-photon ionisation (REMPI) detection of H atoms that reach the target region. A $(2+1)$ REMPI scheme is employed, using the 243 nm output of a frequency-doubled pulsed dye laser.[29] ToF traces are recorded with and without the magnetic guide in place. When the MRF is in place, experiments are conducted with the guide parameters optimised for two different target velocities. The difference in configuration lies primarily in the z-axis separation of the Halbach arrays within each pair. Different velocities are preferentially transmitted with different array separations, as the separation between the arrays in each pair corresponds to a distance of $2f$ (where f is the focal length). Here, the properties of the magnets are such that LFS H atoms travelling at 350 m s^{-1} and 300 m s^{-1} are focused at $f = 12.4$ mm and 9.4 mm (respectively). There is a minor (0.1 mm) difference in the vertical offset of the second pair of Halbach arrays between the two sets of experiments. All other parameters are unchanged between the two magnetic guide configurations.

The experimental and simulated ToF traces are in excellent agreement. When the guide is not in place, the ToF traces simply show the initial velocity distribution of the hydrogen beam. The modal velocity of the H atoms is approximately 500 m s^{-1}, and the ToF traces recorded without the guide are peaked at approximately 570 μs. With the guide in place, the ToF distributions become narrower, peak later (at around 750 μs), and exhibit a lower intensity. These changes arise from the removal of the non-target H atoms from the beam. The peak intensity decreases as the target velocity is reduced from 350 m s^{-1} to 300 m s^{-1} as there are fewer particles travelling at the lower velocity in the incoming beam.

Table I displays the difference in the transmission of H atoms in LFS states travelling at different velocities. The target velocity is defined as 300 ± 10 m s^{-1}; faster particles are those with velocities greater than 310 m s^{-1}, and slower particles have velocities below 290 m s^{-1}. In the initial beam, only 1% of all hydrogen atoms in LFS states are travelling at the target velocity. With the guide in place, 40% of H atoms that reach the detection region are travelling at the target

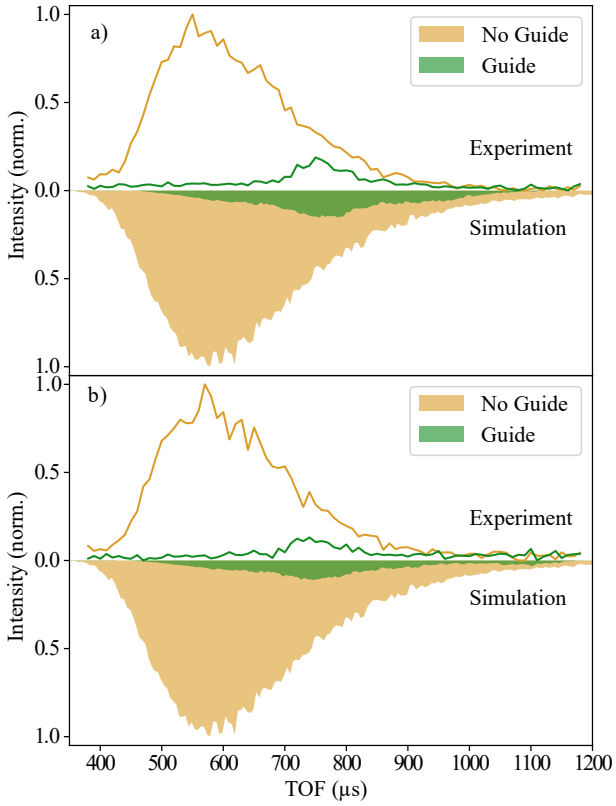

FIG. 2. Experimental and simulated Time-of-Flight (ToF) traces are shown for the H atoms that successfully reach the detection region. Each plot depicts the ToF profile recorded without the magnetic guide ("No Guide") and with the magnetic guide in place ("Guide"), for target velocities of (a) 350 $\mathrm{m\,s^{-1}}$ and (b) 300 $\mathrm{m\,s^{-1}}$.

velocity. The magnetic guide removes 99% of faster H atoms and 96% of slower H atoms in LFS states from the beam. As Figure 3 illustrates, only H atoms travelling at the target velocity arrive at the detector with a y distribution that is symmetric about the beam axis. Faster LFS radicals are deflected downwards, whereas slower LFS radicals are shifted upwards. This indicates that future amendments to the MRF experimental set-up (for example, in the form of an iris in front of the detection region) could achieve a significantly narrower velocity distribution. It should be noted that the choice of target velocity range here is fairly arbitrary; a very narrow target velocity range—as selected here—simply serves to illustrate the effectiveness of the guide.

The way that the various elements of the magnetic guide combine to filter the beam can be seen in the particle trajectory simulations presented in Figure 4. The passage of H atoms in LFS states travelling through the magnetic guide at the target velocity (350 ± 10 $\mathrm{m\,s^{-1}}$), and at velocities above and below this narrow target range, are shown. The majority of radicals travelling at the

TABLE I. The relative amounts of target (300 ± 10 m s^{-1}), slower (< 290 m s^{-1}) and faster (> 310 m s^{-1}) LFS hydrogen atoms in the beam that reach the detection region with and without the magnetic guide in place is shown. With the guide in place, 90% of target particles are transmitted; 99% of faster (and 96% of slower) hydrogen atoms in LFS states are removed from the beam.

% of H atoms in LFS states	Target	Slower	Faster
In transmitted beam (no guide)	1%	1%	98%
In transmitted beam (with guide)	40%	3%	57%
Removed from the beam (with guide)	10%	96%	99%

target velocity are successfully guided around the blades and into the detection region. The majority of faster H atoms are physically blocked by the skimming blades; the small number of faster H atoms in LFS states that make it past the second skimming blade are deflected away from the target region. Slower H atoms in LFS states are over-focused, and most collide with the blades or are deflected away.

The overlapping of the two blades in the y-axis, which leaves no direct line-of-sight through the magnetic guide, is a key feature of the MRF device. All species unaffected by the magnetic fields of the arrays—seed gas particles, precursor molecules, other contaminant species in the beam—are physically blocked by the blades. Particle trajectory simulations indicate that no H atoms in HFS states reach the detection region with the MRF in place. It should be noted that there is no external magnetic field present beyond the last Halbach array. We therefore cannot rule out the possibility of spin flip transitions to other non-LFS states (for example, to $F = 0$) in the ~ 100 μs it takes the beam to travel from the last array into the detection region. To avoid the possibility of any spin flips occurring, and to facilitate the study of spin-polarized hydrogen, a small offset magnetic field could be applied.

Even though the guide removes some 99% of H atoms in LFS states travelling faster than the target species, these faster radicals represent the vast majority of H atoms in the initial distribution. Only 2% of H atoms in the incoming beam have a z velocity ≤ 310 m s^{-1}. As such, the 1% of faster LFS hydrogen atoms that make it to the target region affect the final velocity distribution; average beam velocities of 394 ± 43 and 350 ± 55 m s^{-1} are observed for target velocities of 350 and 300 m s^{-1}, respectively. Straightforward amendments could be made to a second-generation MRF. For example, an additional focusing element could be introduced before the guide; the length

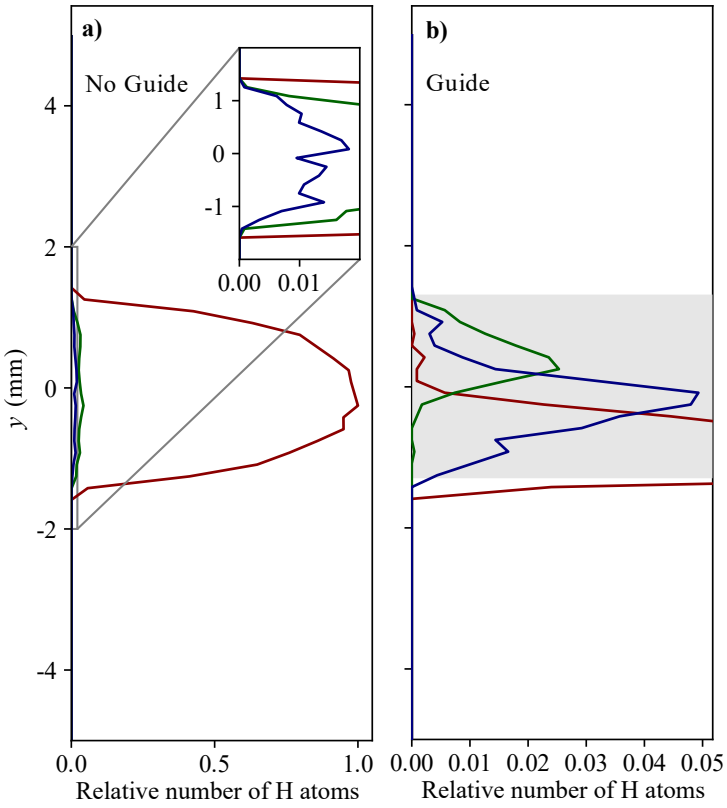

FIG. 3. Simulated distribution of the state-selected H atom beam at the detection region, plotted along the y-axis, (a) without and (b) with the magnetic guide in place. The initial beam of H atoms is centred at y = 0 mm. The vast majority of particles in the non-guided beam are travelling faster than the target velocity, as depicted by the dark red trace. The blue traces represent the distribution of the target species (with a velocity of 350 $\pm$ 10 m s^{-1}). Particles travelling with a velocity below the target range are shown in green. The detection region (defined to match the acceptance of an ion trap) is simulated as a circle with radius 1.3 mm, indicated by the shaded region in plot (b).

of the guide could be extended (so that the same amount of deflection achieves a larger separation of velocities); an additional element such as an iris could be placed in front of the detection region. The resultant stand-alone magnetic guide could act as a versatile filter to generate state-selected beams of a range of radical species with a narrow velocity distribution, directly from an effusive or supersonic source.

To the best of our knowledge, there is no comparable device that offers the same degree of state and velocity selectivity for gas-phase radicals such as H atoms. For example, Zeeman decelerators can generate slow-moving beams of state-selected radicals with a very narrow velocity distribution, but they do not block the passage of any other species through the device. In crossed

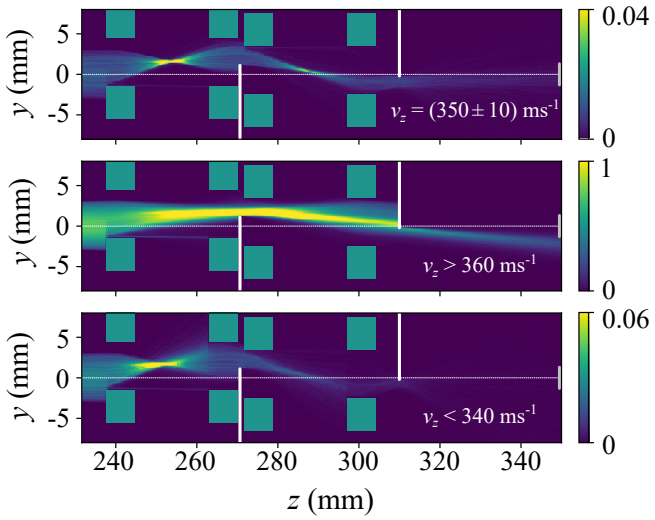

FIG. 4. Three-dimensional particle trajectory simulations of a beam of state-selected H atoms through the guide. The top, middle and bottom panels show the trajectories of LFS particles travelling at the target velocity (350 $\pm$ 10 m s^{-1}), faster than the target velocity range, and slower than the target velocity range, respectively. Beside each panel, colour bars indicate the relative intensities of the particles. The Halbach arrays are represented in cross-section by green rectangles, with the skimming blades depicted by vertical white lines. At z = 350 mm, the small grey region indicates the detection region.

beam experiments, this lack of beam purity is not an issue as the unwanted species typically pass through ahead of the radical species of interest. The second (crossed) beam is timed such that it encounters only the target decelerated species, thereby avoiding any competing side reactions. This approach does not work with an effectively stationary target, and decelerated beams require filtering (with a device such as the MRF)[35] prior to being interfaced with static targets such as ion traps. Bent magnetic guides, such as those cited in the introduction, can produce state-selected radical beams. There is some velocity selectivity with bent guides, as only species travelling below a certain threshold velocity (determined by the radius of the curve and the strength of the guiding fields) make it around the bend. However, the velocity distribution of beams generated by a bent guide can be quite broad and it is typically not possible to tune this range. Combining a straight magnetic guide—such as a magnetic hexapole—with a beam stop has been shown to produce a radical beam with high state selectivity. As the beam stop removes the direct line-of-sight between the source and the detection region, most contaminant species are successfully removed from the beam. Precursor species were found to account for $\leq 7\%$ and $\leq 5\%$ of the post-magnetic hexapole beam in studies of Ar(^{3}P$_2$) and N$_2$(A$^3\Sigma_u^+$) radicals (respectively).[16,17] As demonstrated above, the

MRF achieves complete state selectivity; in this work, only the target radical species reach the detection region.

A further study undertaken with a magnetic hexapole and beam stop apparatus reported the velocity distribution of transmitted He(^{3}S) radicals when different numbers of magnetic hexapole units were in place. While altering the number of hexapole units affected the velocity distribution of the post-hexapole beam, the range of transmitted velocities was found to span several hundred m s^{-1} for each configuration considered.[18] Also, the number of hexapole units in a magnetic hexapole guide can only be adjusted by integer values (*i.e.*, by adding or removing an entire hexapole magnet), and this cannot be altered under vacuum. The MRF presented in this work is continuously tuneable, produces a narrower velocity distribution, and the target velocity can be adjusted without the need to break vacuum. The MRF is also versatile; the Halbach arrays can be swapped for arrays with different properties, enabling radical species other than H atoms to be targeted in future work. (Indeed, the Halbach arrays employed in this study have different properties to those used when the guide was initially employed in combination with a Zeeman decelerator, where slower H atoms were targeted.)[35,36]

IV. CONCLUSIONS

It has been experimentally demonstrated that a magnetic guide can filter the state-selected H atoms of interest from all other components of a beam. No other species—H atoms in non-guided states, or other contaminant species present in the initial beam—are transmitted through to the detection region. The MRF also preferentially transmits H atoms travelling at a selected target velocity. The experimental results are supported by particle trajectory simulations, enabling the properties of the filtered beam to be evaluated. Our calculations indicate that the magnetic guide could be utilised to generate state-selected low-velocity beams of a range of other radical species, such as OH molecules, by including Halbach arrays with different properties. This work presents the first experimental evidence that the MRF can operate as a stand-alone radical beam filter. Following a number of proposed improvements, a second-generation MRF (specifically designed to operate as a stand-alone device) is expected to achieve even greater velocity selectivity and versatility.

ACKNOWLEDGMENTS

J.T. gratefully acknowledges the EPSRC for a Doctoral Prize Award and the Lindemann Trust for a Postdoctoral Fellowship. B.R.H. thanks the Engineering and Physical Sciences Research Council (EPSRC, EP/N032950/1 and EP/N004647/1) and the Royal Society (RGS\R2\192210) for financial support.

DATA AVAILABILITY

The data that support the findings of this study are available from the Oxford Research Archive.

REFERENCES

[1]J. Thiebaud, A. Aluculesei, and C. Fittschen, "Formation of HO_2 radicals from the photodissociation of H_2O_2 at 248 nm," The Journal of Chemical Physics **126**, 186101 (2007).

[2]L. Ghassemzadeh, T. J. Peckham, T. Weissbach, X. Luo, and S. Holdcroft, "Selective formation of hydrogen and hydroxyl radicals by electron beam irradiation and their reactivity with perfluorosulfonated acid ionomer," Journal of the American Chemical Society **135**, 15923–15932 (2013).

[3]J. Slevin and W. Stirling, "Radio frequency atomic hydrogen beam source," Review of Scientific Instruments **52**, 1780–1782 (1981).

[4]W. Gerlach and O. Stern, "Der experimentelle nachweis des magnetischen moments des silberatoms," Zeitschrift für Physik **8**, 110–111 (1922).

[5]W. Gerlach and O. Stern, "Der experimentelle nachweis der richtungsquantelung im magnetfeld," Zeitschrift für Physik **9**, 349–352 (1922).

[6]G. Breit and I. I. Rabi, "Measurement of nuclear spin," Physical Review **38**, 2082–2083 (1931).

[7]I. I. Rabi and V. W. Cohen, "Measurement of nuclear spin by the method of molecular beams. The nuclear spin of sodium," Physical Review **46**, 707–712 (1934).

[8]J. M. B. Kellogg, I. I. Rabi, N. F. Ramsey Jr., and J. R. Zacharias, "The magnetic moments of the proton and the deuteron. The radiofrequency spectrum of H_2 in various magnetic fields," Physical Review **56**, 728–743 (1939).

[9]K. Halbach, "Design of permanent multipole magnets with oriented rare earth cobalt material," Nuclear Instruments and Methods **169**, 1–10 (1980).

[10]B. Ghaffari, J. M. Gerton, W. I. McAlexander, K. E. Strecker, D. M. Homan, and R. G. Hulet, "Laser-free slow atom source," Physical Review A **60**, 3878–3881 (1999).

[11]A. Goepfert, F. Lison, R. Schütze, R. Wynands, D. Haubrich, and D. Meschede, "Efficient magnetic guiding and deflection of atomic beams with moderate velocities," Applied Physics B: Lasers and Optics **69**, 217–222 (1999).

[12]M. Greiner, I. Bloch, T. W. Hänsch, and T. Esslinger, "Magnetic transport of trapped cold atoms over a large distance," Physical Review A **63**, 031401(R) (2001).

[13]K. Dulitz and T. P. Softley, "Velocity-selected magnetic guiding of Zeeman-decelerated hydrogen atoms," The European Physical Journal D **70**, 19 (2016).

[14]K. Hayashi, N. Sakudo, T. Noda, A. Takeda, K. Fujimura, and N. Shimizu, "A new method for generating a refined beam of neutral radicals," Nuclear Instruments and Methods in Physics Research Section B: Beam Interactions with Materials and Atoms **127**, 918–921 (1997).

[15]G. Borodi, A. Luca, and D. Gerlich, "Reactions of CO_2^+ with H, H_2 and deuterated analogues," International Journal of Mass Spectrometry **280**, 218–225 (2009).

[16]D. Watanabe, H. Ohoyama, T. Matsumura, and T. Kasai, "Steric effect in the energy transfer reaction of Ar ($^3P_2$) + N_2," The Journal of Chemical Physics **125**, 084316 (2006).

[17]H. Ohoyama and S. Maruyama, "Alignment effect of N_2 ($A^3\Sigma_u^+$) in the energy transfer reaction of aligned N_2 ($A^3\Sigma_u^+$) + NO ($X^2\Pi$) $\rightarrow$ NO ($A^2\Sigma^+$) + N_2 ($X^1\Sigma_g^+$)," The Journal of Physical Chemistry A **116**, 6685–6692 (2012).

[18]D. Watanabe, H. Ohoyama, T. Matsumura, and T. Kasai, "Characterization of an oriented metastable atom source based on a magnetic hexapole," The European Physical Journal D - Atomic, Molecular, Optical and Plasma Physics **38**, 219–223 (2006).

[19]M. Kirste, H. Haak, G. Meijer, and S. Y. T. van de Meerakker, "A compact hexapole state-selector for NO radicals," Review of Scientific Instruments **84**, 073113 (2013).

[20]M. C. van Beek, J. J. ter Meulen, and M. H. Alexander, "Rotationally inelastic collisions of OH($X^2\Pi$) + Ar. I. State-to-state cross sections," The Journal of Chemical Physics **113**, 628–636 (2000).

[21]C. J. Eyles, M. Brouard, H. Chadwick, B. Hornung, B. Nichols, C.-H. Yang, J. Kłos, F. J. Aoiz, A. Gijsbertsen, A. E. Wiskerke, and S. Stolte, "Fully Λ-doublet resolved state-to-state differential cross-sections for the inelastic scattering of NO(X) with Ar," Phys. Chem. Chem. Phys. **14**, 5403–5419 (2012).

[22]N. Vanhaecke, U. Meier, M. Andrist, B. H. Meier, and F. Merkt, "Multistage Zeeman deceleration of hydrogen atoms," Physical Review A **75**, 031402 (2007).

[23]E. Narevicius, C. G. Parthey, A. Libson, J. Narevicius, I. Chavez, U. Even, and M. G. Raizen, "An atomic coilgun: using pulsed magnetic fields to slow a supersonic beam," New Journal of Physics **9**, 358 (2007).

[24]E. Narevicius, A. Libson, C. G. Parthey, I. Chavez, J. Narevicius, U. Even, and M. G. Raizen, "Stopping supersonic beams with a series of pulsed electromagnetic coils: an atomic coilgun," Physical Review Letters **100**, 093003 (2008).

[25]A. W. Wiederkehr, S. D. Hogan, and F. Merkt, "Phase stability in a multistage Zeeman decelerator," Physical Review A **82**, 043428 (2010).

[26]A. W. Wiederkehr, M. Motsch, S. D. Hogan, M. Andrist, H. Schmutz, B. Lambillotte, J. A. Agner, and F. Merkt, "Multistage Zeeman deceleration of metastable neon," The Journal of Chemical Physics **135**, 214202 (2011).

[27]E. Lavert-Ofir, S. Gersten, A. B. Henson, I. Shani, L. David, J. Narevicius, and E. Narevicius, "A moving magnetic trap decelerator: a new source of cold atoms and molecules," New Journal of Physics **13**, 103030 (2011).

[28]T. Momose, Y. Liu, S. Zhou, P. Djuricanin, and D. Carty, "Manipulation of translational motion of methyl radicals by pulsed magnetic fields," Physical Chemistry Chemical Physics **15**, 1772–1777 (2013).

[29]K. Dulitz, M. Motsch, N. Vanhaecke, and T. P. Softley, "Getting a grip on the transverse motion in a Zeeman decelerator," The Journal of Chemical Physics **140**, 104201 (2014).

[30]M. Motsch, P. Jansen, J. A. Agner, H. Schmutz, and F. Merkt, "Slow and velocity-tunable beams of metastable He_2 by multistage Zeeman deceleration," Physical Review A **89**, 043420 (2014).

[31]J. Toscano, A. Tauschinsky, K. Dulitz, C. J. Rennick, B. R. Heazlewood, and T. P. Softley, "Zeeman deceleration beyond periodic phase space stability," New Journal of Physics **19**, 083016 (2017).

[32]T. Cremers, S. Chefdeville, V. Plomp, N. Janssen, E. Sweers, and S. Y. T. van de Meerakker, "Multistage Zeeman deceleration of atomic and molecular oxygen," Physical Review A **98**, 033406 (2018).

[33]J. Toscano, L. Y. Wu, M. Hejduk, and B. R. Heazlewood, "Evolutionary algorithm optimization of Zeeman deceleration: Is it worthwhile for longer decelerators?" The Journal of Physical Chemistry A **123**, 5388–5394 (2019).

[34]V. Plomp, Z. Gao, T. Cremers, M. Besemer, and S. Y. T. van de Meerakker, "High-resolution imaging of molecular collisions using a Zeeman decelerator," The Journal of Chemical Physics **152**, 091103 (2020).

[35]J. Toscano, C. J. Rennick, T. P. Softley, and B. R. Heazlewood, "A magnetic guide to purify radical beams," The Journal of Chemical Physics **149**, 174201 (2018).

[36]J. Toscano, M. Hejduk, H. G. McGhee, and B. R. Heazlewood, "Manipulating hydrogen atoms using permanent magnets: Characterisation of a velocity-filtering guide," Review of Scientific Instruments **90**, 033201 (2019).